Astron. Astrophys. 344, 154–162 (1999)

ASTRONOMY AND ASTROPHYSICS

Rotational modulation of X-ray flares on late-type stars: T Tauri stars and Algol

B. Stelzer[1], **R. Neuhäuser**[1], **S. Casanova**[2], **and T. Montmerle**[2]

[1] Max-Planck-Institut für Extraterrestrische Physik, Giessenbachstrasse 1, D-85740 Garching, Germany
[2] Service d'Astrophysique, CEA Saclay, F-91191 Gif-sur-Yvette, France

Received 23 October 1998 / Accepted 18 December 1998

Abstract. We present evidence for rotational modulation of X-ray flares by an analysis of four outbursts on late-type stars. Two of the flares we discuss are found in *ROSAT* observations of T Tauri Stars and were obtained between September and October 1991. A flare on the T Tauri Star V773 Tau was observed by *ASCA* in September 1995. To this sample we add a *Ginga* observation of a flare on Algol observed in January 1989.

The structure of the X-ray lightcurves observed in this selection of flare events is untypical in that the maximum emission extends over several hours producing a round hump in the lightcurve instead of a sharp peak. We explain this deviation from the standard shape of a flare lightcurve as the result of a flare erupting on the back side of the star and gradually moving into the line of sight due to the star's rotation. Making use of the known rotational periods of the stars our model allows to determine the decay timescale of the flares and the size of the X-ray emitting volume according to the standard magnetic loop model. Spectral information, which is available in sufficient quality for the Algol observation only, supports our proposition that changes of the visible volume are responsible for the observed time development of these flares.

Key words: X-rays: stars – stars: rotation – stars: late-type – stars: individual: SR 13, P1724, V773 Tau, Algol – stars: flare

1. Introduction

After the first stellar X-ray flares were discovered less than 25 years ago on dMe stars (Heise et al. 1975) it took almost another decade until the *Einstein observatory* (*EO*) detected similar events on young T Tauri Stars (TTS) (Montmerle et al. 1983). Nowadays, X-ray flares are known to be entertained on stars all over the H-R diagram (see Pettersen 1989 for a review). The timescales and energetics involved in flare events on different types of stars vary strongly consistent with the observation that the level of X-ray activity decays with age.

TTS are late-type pre-main sequence stars with typical age of 10^5–10^7 yrs and rank among the most active young stars: energy outputs of up to 10^4 times the maximum X-ray emission observed from solar flares have been reported from TTS outbursts. Some of the largest X-ray flares ever observed were discovered by *ROSAT* on the TTS LHα 92 and P1724 (Preibisch et al. 1993, Preibisch et al. 1995). The energy released in these events ($> 10^{36}\,\mathrm{ergs}$) exceeds that of typical TTS flares by two orders or magnitude. Before the detection of these giant events, the record of X-ray luminosity was held for more than 10 years by the TTS ROX-20, where $L_\mathrm{x} \sim 10^{32}\,\mathrm{ergs/s}$ were measured during an *EO* observation in February 1981 (Montmerle et al. 1983). A superflare from the optically invisible infrared Class I protostar YLW 15 in ρ Oph was presented by Grosso et al. (1997), with the intrinsic X-ray luminosity over the whole energy range being 10^{34} to 10^{36} erg/s, depending on the foreground absorption which is known to lie somewhere between 20 and 40 mag.

Although no model has been found yet that explains all aspects of flaring activity, the basic picture of all flare scenarios is – in analogy to the sun – that of dynamo driven magnetic field loops that confine a hot, optically thin, X-ray emitting plasma (see Haisch et al. 1991 for a summary of flare phenomena). Quasi-static cooling of such coronal loops has been described by van den Oord & Mewe (1989). An analysis of single flare events is of interest to determine physical parameters of the flaring region such as time scales, energies, temperature and plasma density, and ultimately decide whether coronal X-ray emission of TTS is scaled-up solar activity, or whether interaction between the star and either a circumstellar disk or a close binary companion are partly responsible for the X-ray emission.

In this paper we select a sample of four X-ray observations (three of TTS and one of Algol) which are in conflict with the standard modeling of the lightcurve as either a flare characterised by a quick rise and subsequent exponential decay or as simple sine-like rotational modulation of the quiescent emission. In the latter case X-ray emission would be larger when the more X-ray luminous area is on the front side of the star (directed towards the observer). Such kind of rotationally modulated emission was observed in the TTS SR 12 in ρ Oph by Damiani et al. (1994).

We propose that the untypical shape of the X-ray lightcurves we present is due to a flare event modulated by the rotation of the star. Skinner et al. (1997) suggested rotational occultation of an X-ray flare to explain the broad maximum and slow decay of a

Send offprint requests to: B. Stelzer (stelzer@xray.mpe.mpg.de)
Correspondence to: B. Stelzer

Table 1. Flare observations

Star	Instrument	Principal Investigator	date [UT]	time [ksec]
Algol	*Ginga* LAC	Stern, R. A.	12-14 Jan 89	37.9
SR 13	*ROSAT* PSPC	Montmerle, T.	07/08 Sep 91	19.9
P1724	*ROSAT* HRI	Caillault, J. P.	02/03 Oct 91	28.1
V773 Tau	*ASCA* SIS0	Skinner, S. L.	16/17 Sep 95	19.8

flare on V773 Tau observed by *ASCA*. While they model their data by fitting a sine function to the lightcurve without allowing for an exponential decay phase (similar to Damiani et al. 1994), we start out from a decaying flare and modify it by a time varying volume factor. By this approach we take into consideration that the flare might be occulted by the star during part of the observation and we are able to estimate the decay timescale of the lightcurve τ and the size of the emitting loop. Such a model was first suggested by Casanova (1994), and Montmerle (1997) classified the corresponding flare event as 'anomalous'. A rotationally modulated flare was also mentioned as possible interpretation of a flare-like event in P1724 (Neuhäuser et al. 1998), shown in our Fig. 6, who advertised the more detailed and quantitative treatment that we present in this paper.

The outline of our presentation is as follows: In Sect. 2 we introduce the X-ray observations that we chose in view of the untypical broad maximum of their lightcurves. A model that describes modulations of X-ray flares by the rotation of the star is presented in Sect. 3. In Sect. 4 we explain the structure of the lightcurves from the observations introduced in Sect. 2 by applying our model, and we summarize the results in Sect. 5.

2. The observations

A summary of the observations analysed in this paper is given in Table 1. The observations were obtained with different instruments onboard the X-ray satellites *ROSAT*, *Ginga*, and *ASCA*. For information about the *ROSAT* instruments, the Position Sensitive Proportional Counter (PSPC) and the High Resolution Imager (HRI), we refer to Trümper (1982). The *Ginga* Large Area Counter (LAC) has been described by Turner et al. (1989), and a description of *ASCA* and its instrumentation can be found in Tanaka et al. (1994).

The classical TTS (CTTS) SR 13 was detected in X-rays by Montmerle et al. (1983). It is located in the $\rho\,\mathrm{Oph}$ cloud at position $\alpha_{2000} = 16^{\mathrm{h}}28^{\mathrm{m}}45^{\mathrm{s}}.3$, $\delta_{2000} = -24^{\circ}28'17.0''$. On a speckle imaging survey SR 13 was discovered to be a binary system (Ghez et al. 1993) with $0.4''$ separation, which remains unresolved in the PSPC observation of 1991 September 07/08 we present here. The period of SR 13 is unknown. However, as shown below, a period of $\sim$ 3–6 days is consistent with the rotating X-ray flare model.

P1724 is a weak line TTS (WTTS) located 15 arc min north of the Trapezium cluster in Orion ($\alpha_{2000} = 5^{\mathrm{h}}35^{\mathrm{m}}4^{\mathrm{s}}.21$, $\delta_{2000} = -5^{\circ}8'13''.2$). Neuhäuser et al. (1998) confirm the rotational period of 5.7 d first discovered by Cutispoto et al. (1996) applying two independent numerical period search methods on the V-band lightcurve. In addition, they report systematic variations of the X-ray count rate of P1724 during an observation with the *ROSAT* HRI in October 1991. However, they cannot find any rotational modulation in the X-ray data. Neuhäuser et al. (1998) also find no indications for a circumstellar disk nor a close binary companion.

The WTTS V773 Tau is a double-lined spectroscopic binary (Welty 1995) which is located in the Barnard 209 dark cloud at optical position ($\alpha_{1950} = 4^{\mathrm{h}}11^{\mathrm{m}}07.29^{\mathrm{s}}$, $\delta_{1950} = 28^{\circ}04'41.2''$). Upper limits for the rotation period derived by Welty (1995) are $2.96\,\mathrm{d}$ and $2.89\,\mathrm{d}$ for the K2 and K5 components respectively. These estimates are somewhat lower than the values previously reported by Rydgren & Vrba (1983). In the *ASCA* observation obtained on 1995 September 16/17 the V773 Tau binary system is not resolved from the classical TTS (CTTS) FM Tau, which lies at an offset of $\sim 38''$. For a more detailed discussion of this *ASCA* observation we refer to Skinner et al. (1997).

Algol is a triple system, with an inner close binary of period 2.87 d comprising a B8 V primary (Algol A) and an evolved K2 IV secondary (Algol B). In January 1989 *Ginga* observed a large flare from the Algol system (presumably Algol B; Stern et al. 1992). The shape of the Algol lightcurve resembles that of the TTS flares discussed before. Therefore, we decided to include this observation in our sample, although the Algol system represents a different class of flare stars.

We use the Extended Scientific Software Analysis System (EXSAS, Zimmermann et al. 1995) to analyse the two *ROSAT* observations, which were obtained from the *ROSAT* Public Data Archive. To take account of possible time variations in the background, the background count rate was computed for each satellite orbit and subtracted accordingly from the measured lightcurve. *Ginga* data were kindly supplied to us in computer readable format by Bob Stern, while Steve Skinner provided us the *ASCA* lightcurve of V773 Tau.

3. Rotational effects on flare lightcurves and spectra

The X-ray lightcurve during a flare event is commonly described by a steep, linear rise followed by an exponential decay. The e-folding time τ of the decay varies greatly between several minutes to hours depending on the nature of the flaring star. Disagreement prevails on the question whether the apparent quiescent emission might be attributed to continuous, unresolved short timescale activity. The detection of a high temperature spectral component in the quiescent spectrum might hint at such low-level flaring (Skinner et al. 1997).

Several flares have been observed that do not match the typical appearance: instead of displaying a sharp peak, the lightcurves of this type of events are characterized by smooth variations around maximum emission that sometimes goes along with a slower rise as compared to standard flare events. In these cases the shape of the lightcurve can be reproduced by taking account of the rotation of the star. Flares that erupt on the backside of the star become visible only gradually as the star rotates and drags the plasma loop around. The visible flare vol-

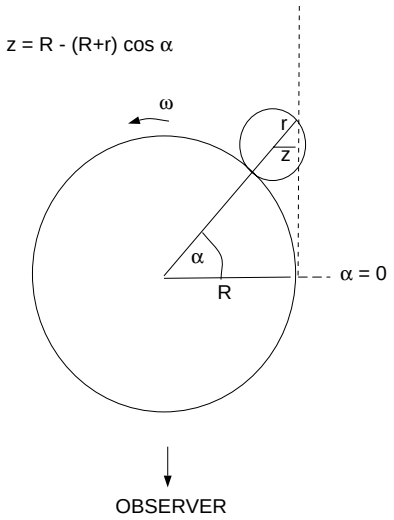

Fig. 1. Top-view of the rotational plane of a flaring star. R is the radius of the star which rotates counterclockwise with angular velocity ω. The flaring volume is represented by the smaller circle of radius r. The angle $\alpha(t)$ is defined to be zero at the time when the plasma loop starts to disappear from the observer's view as a consequence of the rotation of the star.

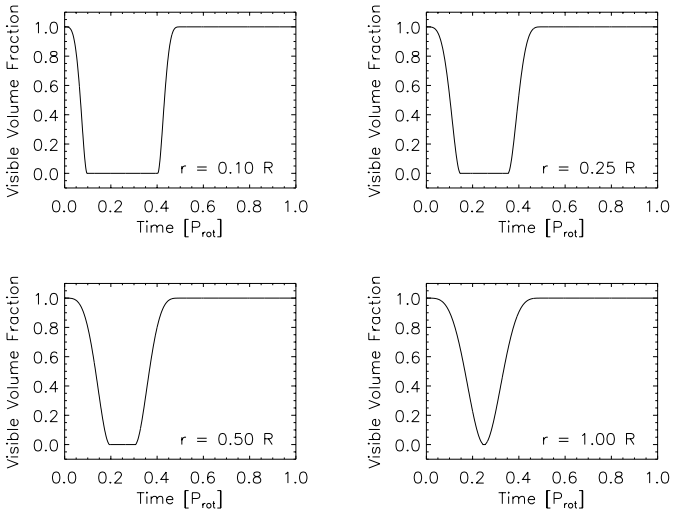

Fig. 2. Visible fraction of the plasma loop volume approximated by our rotating-flare model of Fig. 1 as a function of time for different values of the radius fraction $f = \frac{r}{R}$.

ume is thus a function of time which modulates the exponential decay. The scenario we have in mind, and that we will refer to as the 'rotating flare model' henceforth, is sketched in Fig. 1.

For simplicity the emitting plasma loop is approximated by a sphere anchored on the star's surface. The fraction of the loop volume which is visible to the observer is given by

$$V(r,t) = \frac{1}{\frac{4}{3}\pi r^3} \int_{R-(R+r)\cdot\cos\alpha(t)}^{r} \pi(r^2 - x^2)\,\mathrm{d}x \qquad (1)$$

where R is the radius of the star and r the radius of the spherical plasma loop. The time dependency of V is hidden in α, the angle between the current position of the flaring volume and the position where a flare just begins to become occulted by the star. Note that Eq. (1) does not hold for rotational phases during which the flaring volume is either completely behind ($\alpha \sim \frac{\pi}{2}$) or completely in front of the star ($\alpha \in [\pi, 2\pi]$). The time dependency of α in Eq. (1) depends on whether the loop is disappearing or reappearing and is given by

$$\alpha(t) = \begin{cases} \frac{2\pi t}{P_{\mathrm{rot}}} & \text{for } 0 \le \alpha(t) < \phi_{\mathrm{crit}}(f) \\ \pi - \frac{2\pi t}{P_{\mathrm{rot}}} & \text{for } \pi - \phi_{\mathrm{crit}}(f) < \alpha(t) \le \pi \end{cases} \qquad (2)$$

where ϕ_{crit} is the critical phase at which the plasma volume has just disappeared. Eq. (1) is not valid any more until the loop reaches phase $\pi - \phi_{\mathrm{crit}}$ and begins to move into the line of sight again. ϕ_{crit} is a function of the relative size of the radius of the flaring volume and the radius of the star, $f = \frac{r}{R}$. The visible fraction of the plasma volume as a function of time is plotted for different values of the radius ratio f in Fig. 2.

Our model is based on several simplifying assumptions concerning the flare geometry. First, we imply that we look directly onto the rotational plane, i. e. $i \sim 90°$, and that the flare takes place at low latitudes. Flares that erupt in polar regions, in contrast, in the configuration of Fig. 1 would remain partially visible during the whole rotation period. Furtheron, Eq. (1) does not take account of the curvature of the star. We content ourselves with these approximations because, given the present quality of the data, further sophistication of the model seems to be unnecessary.

Making use of the configuration described above, for a flare which is observed while the flaring region turns up from the backside of the star, the X-ray lightcurve can be modeled by

$$I_{\mathrm{cps}} = I_{\mathrm{q}} + I_0 \cdot \exp(-t/\tau) \cdot V(r,t) \qquad (3)$$

where I_{q} is the quiescent X-ray count rate of the star, I_0 the strength of the outburst, τ the decay timescale of the count rate and $V(r,t)$ the visible fraction of the volume of the plasma loop given by Eq. (1) for values of α within the allowed range, and by 0 or 1 for angles α outside the intervals of Eq. (2).

The hump-like shape of the lightcurves we will discuss in the next section can be reproduced if the visible volume V *increases* during the first *observed* part of the flare, ie. $\alpha \ge \pi - \phi_{\mathrm{crit}}$. Three critical moments determine the rotating flare event: the time of outburst, the time when the flare region passes phase $\pi - \phi_{\mathrm{crit}}$ and begins to move into the line of sight, and the time at which the observation started. In the next paragraphs the relation between these times will be examined.

First, an offset between flare outburst and the time when it becomes visible to an observer (at $\pi - \phi_{\mathrm{crit}}$) might be present, when the flare takes place on the occulted side of the star. In our model such a time offset Δt contributes only to the normalization of the exponential $I_0 = I_{\mathrm{intr}} \cdot \exp(-\Delta t/\tau)$ and cannot be separated from the intrinsic brightness I_{intr} of the outburst. The upper limit for Δt is given by

$$\Delta t_{\max} = (0.5\text{–}2\phi_{\mathrm{crit}}) P_{\mathrm{rot}} \qquad (4)$$

since for larger time offsets the flare would have been observed also at $\alpha < \phi_{\mathrm{crit}}$, that is before its occultation. Given the rotational periods of several days, $\Delta t_{\max}$ exceeds the typical decay

timescale for TTS flares (of a few hours). However, from an observational point of view it is impossible to exclude that the flares occurred already before they rotated away, because data extending over several hours before the reappearance of the flare are not available for the lightcurves analysed here, except in the case of Algol. Indeed, at first glance the combination of the two phases of enhanced count rate in the Algol observation (see Fig. 3a) looks similar to what is expected to be seen from *one* very long flare that disappeared behind the star shortly after outburst and reappeared half a rotational cycle later still displaying a strong count rate enhancement. Fig. 3b gives an example of a theoretical lightcurve for a flare which is occulted right after its outburst and whose duration is more than half the rotation period. However, our attempt to model the complete Algol lightcurve from Fig. 3a by such a single temporary occulted flare was not successful because the model restrictions concerning the relative strength of the pre- and post-occultation part of the flare are not met by the Algol lightcurve. Thus we can rule out offsets larger than $\Delta t_{\max}$ for the Algol observation discussed in this paper, and the short rise in count rate observed before the large flare must be due to an independent event.

Second, the start of the observation of a flare event, which is characterised by a beginning enhancement of the observed count rate, can differ from the time at which the outer edge of the plasma loop emerges from the back of the star due to gaps in the data stream. So, strictly speaking, another offset δt has to be included when fitting the 'rotating flare model' to the data to take account of a possible delay of the observation with respect to flare phase $\pi - \phi_{\rm crit}$. Such an additional parameter that allows to determine the rotational phase of the flare region at the beginning of the observed rise is needed to obtain acceptable fits for the flares on Algol and V773 Tau. For the *ROSAT* observations (of SR 13 and P1724), however, an offset δt does not improve the fit due to the low statistics of the data. We note here, that the observed flare rise is only *apparent* according to our model: The star is assumed to have flared (and thus exhibited its maximum emission) well before the *observed* maximum, and the count rate is low at that time only due to the fact that the flaring volume has not yet become visible.

The enhanced X-ray emission during flare events is produced by a hot plasma which has been heated to temperatures of 10^6 K and above. Optically thin plasma models show, when applied to spectra representing different stages of the flare, that after the outburst the temperature drops exponentially to the quiescent level. The temperature observed for a rotationally modulated flare should thus be highest during the phase where the flare emerges from the backside of the star when the observed lightcurve has not yet reached its maximum. The emission measure, on the other hand, being a volume related parameter is expected to show a time evolution similar to the lightcurve.

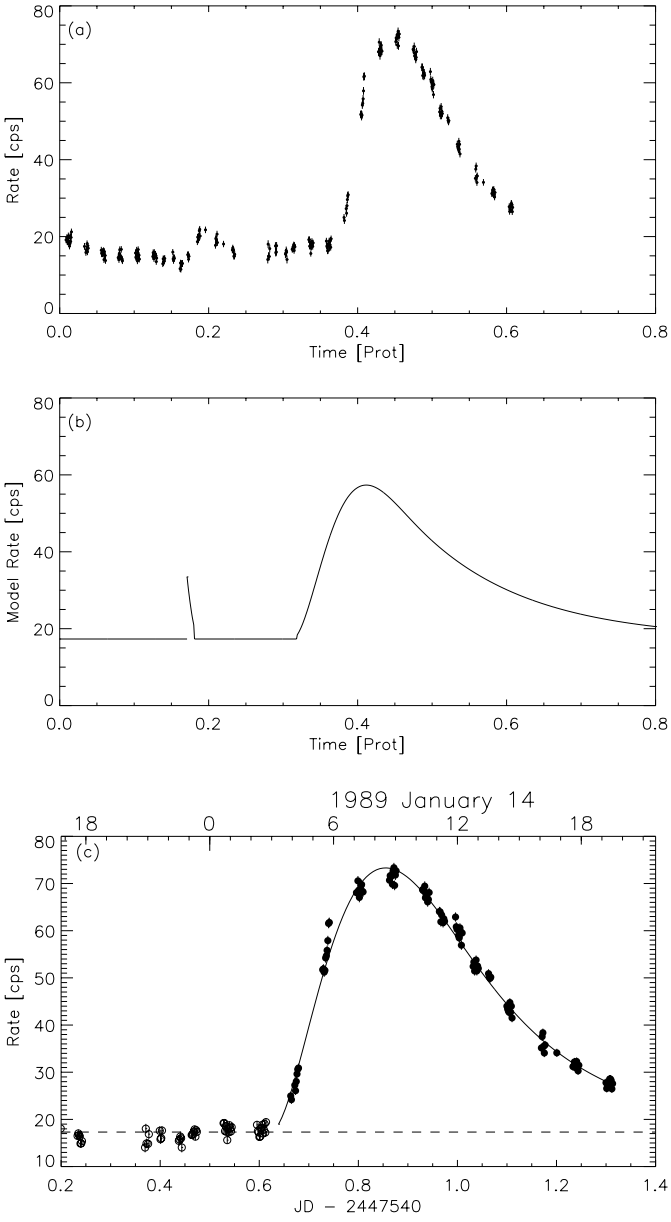

Fig. 3a–c. *GINGA* lightcurve of the Algol flare in comparison with the rotating-flare model: **a** Algol lightcurve including the short event 13 hours before the large flare, **b** theoretical shape of a lightcurve representing a strong flare which is occulted immediately after its outburst and reappears later, and **c** large Algol flare overlaid by our best fit model curve. Binsize: 128 s (1 σ uncertainties)

4. Application of the model

We fit the model of Eq. (3) to that part of the lightcurves from the observations introduced in Sect. 2 that are by visual inspection identified with the outburst due to their enhanced count rates. Except for V773 Tau (see Fig. 7) none of these lightcurves (Fig. 3c, Fig. 5, and Fig. 6) can be explained by simple sine-like variations due to rotational modulation of the quiescent emission. There is always an additional feature present, namely a flare. The lightcurves discussed here are characterised by a concave shape of the (e-folding) decay phase typical for flares (whether or not rotationally modulated), while a simple sine-like rotational modulation of quiescent emission always produces a convex shape in the decay part.

In all cases we examined, the quiescent count rate is held fixed on its average pre-flare value. Thus, three free parameters have to be adjusted to the data: the strength of the flare, I_0 in cts/s, the decay timescale of the lightcurve, τ, and the radius r of the flaring volume relative to the stellar radius, R. An additional freedom allowing for an offset δt between rotational phase $\pi - \phi_{\rm crit}$ of the flare and the *apparent* outburst of the flare, which is observed as a rise in count rate, is used for the modeling of the *Ginga* (Algol) and *ASCA* (V773 Tau) lightcurves (see the explanation in the previous section).

The rotational periods $P_{\rm rot}$ of our sample stars were known from optical photometry, except for the case of SR 13. In principle, $P_{\rm rot}$ could be included as a further free parameter in the fit. But with this additional freedom the fit does not result in a unique solution, as we will show in the example of SR 13, and thus $P_{\rm rot}$ may not be uniquely determined from our model. For Algol we assume synchronous rotation.

Our best fit results will be discussed in detail in the following subsections. The best fit parameters for all flares are listed in Table 2 together with the rotation periods and measured quiescent count rates. Note, however, that the model depends to some degree on the initial parameters, and the parameters are not well determined due to correlations, such that similar solutions are obtained for different combinations of parameter values. For the flares on Algol and V773 Tau we computed 90 % confidence levels for the best fit parameters according to the method described by Lampton et al. (1976). The low statistics in the data of the lightcurves of SR 13 and P 1724 do not allow to apply this method. We, therefore, do not give uncertainties for the best fit parameters of these events.

4.1. Algol

A two day long continuous *Ginga* observation of Algol in January 1989 (first presented by Stern et al. 1990, 1992) includes a large flare event. Secondary eclipse begins during the decay of that flare, but it seems to affect the count rate only marginally. Preceding the large flare, primary eclipse and a small flare are observed (see discussion in Sect. 3). We therefore base our estimate for the quiescent emission on the time between the two flare events, i.e. immediately before the rise phase of the large outburst which marks the onset of the time interval to which we apply the 'rotating-flare model'. From fitting Eq. (3) to the data after JD 2447540.65 in Fig. 3c we obtain a best fit $\chi^2_{\rm red}$ of 5.34 for 108 degrees of freedom. The fit can be significantly improved when the critical phase $\pi - \phi_{\rm crit}$ is allowed to vary around the start of observation as explained in Sect. 3 ($\chi^2_{\rm red} = 3.05$ for 107 dofs), and all stages of the flare are well represented by the model. Although this value of $\chi^2_{\rm red}$ is still far from representing an excellent fit, the ability of the model to reproduce the overall shape of the X-ray lightcurve is convincing.

A detailed spectral analysis of the flare event on Algol was undertaken by Stern et al. (1992). The emission measure EM they obtained from a thermal bremsstrahlung spectrum + Fe line emission for 11 time-sliced spectra covering all phases of the flare is displayed in Fig. 4. According to the best fit of our 'rotating flare model' to the lightcurve, the flare volume has become almost completely visible ($V > 0.98$) around JD 2447541, i.e. about 10 hours after the rise in count rate was observed to set in. The exponential decay of the emission measure for the last three values of Fig. 4 can thus be extrapolated to the previous part of the observation to find the values for the emission measure intrinsic to this flare event. The observed emission measure during the rotationally dominated beginning of the flare is then fairly well reproduced by correcting the extrapolated values for the time dependence of the volume ($EM \sim n_{\rm e}^2 V$), where we neglect possible variations of the plasma density $n_{\rm e}$. Thus, in contrast to the observation, the actual emission measure of the flare event is highest at the onset of the flare at JD ~ 2447540.6 and it decays simultaneously with the count rate ($\tau_{\rm EM} = 6.45 \pm 0.67\,{\rm h}$) due to a decrease of $n_{\rm e}$ or shrinking loop volume. The good agreement between the emission measure observed by Stern et al. (1992) and the values expected from our model (see Fig. 4) provide convincing evidence that the application of the 'rotating-flare model' is justified for this flare. The development of the temperature during the flare (see Stern et al. 1992) does not show the characteristic hump shape, but is close to a pure exponential decay as expected for volume unrelated parameters.

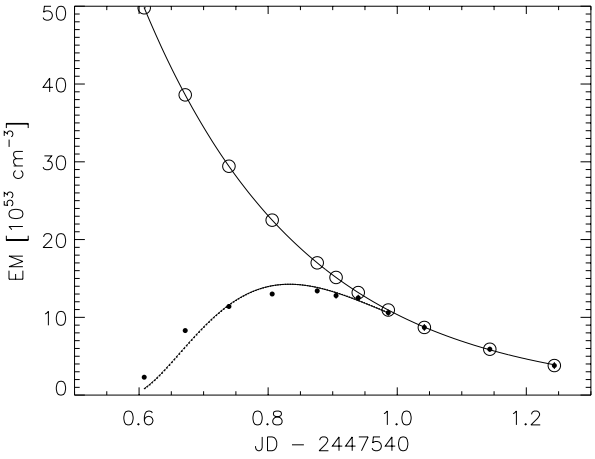

Fig. 4. Emission measure during the large flare on Algol. Small, filled circles represent the spectral results of Stern et al. (1992). Large, open circles are our extrapolation of the exponential decay fitted to the last three data points of Stern et al. (1992). The lower curve denotes the extrapolated emission measure after correction for the time dependence of the volume.

The values of the flare parameters (τ, r) resulting from the fit of our model to the lightcurve are similar to those derived from normal (ie. neither occulted nor rotationally modulated) Algol flares observed by various instruments. Ottmann et al. (1996) summarize the characteristic parameters of three Algol flares (see their Table 5): the decay timescale seems to vary by one order of magnitude between ~ 3 and ~ 36 hours, while the loop length found from standard loop modeling extends from ~ 0.5–2 stellar radii. We conclude that modelling the January 1989 X-ray flare on Algol in terms of rotational modulation

Table 2. Best fit parameters of the rotating-flare model and 1 σ uncertainties. No uncertainties are given for the *ROSAT* observations (see text). Dots indicate that no uncertainties could be determined within the limits of the parameters given by model restrictions (ie. $0 < r < 1$).The rotational periods were fixed on the values given in column 2 except for SR 13 whose rotational period is unknown: [a] Hill et al. 1971 (assuming synchronous rotation of Algol B), [b] Cutispoto et al. 1996, and [c] Welty 1995. The quiescent count rate, $I_{\rm q}$, was determined from the pre-flare data except for V773 Tau.

Star	$P_{\rm rot}$ [d]	$I_{\rm q}$ [cps]	I_0 [cps]	τ [h]	r [R_*]	δt [h]	$\chi^2_{\rm red}$ (dof)
Algol	2.87^a	17.32 ± 0.02	$207.8^{+72.2}_{-64.1}$	$5.2^{+0.1}_{-0.4}$	$0.55^{+\dots}_{-0.12}$	$0.6^{+0.8}_{-0.1}$	3.05 (107)
SR 13	3	0.03	0.58	4.1	0.65		1.23 (36)
	6	0.03	2.58	2.9	0.65		1.16 (36)
P1724	5.7^b	0.04	0.25	4.8	0.10		0.99 (36)
V773 Tau*	2.97^c	0.10 ± 0.02	$2.1^{+1.1}_{-0.6}$	$21.9^{+7.8}_{-8.3}$	$0.22^{+\dots}_{-\dots}$	$3.9^{+\dots}_{-2.1}$	1.45 (149)

* Fit includes an additional X-ray emitting region (see text)

yields flare properties which are perfectly consistent with those of other X-ray flares.

4.2. SR 13

Casanova (1994) discusses the similarity between a flare of SR 13 observed by the *ROSAT* PSPC and the Algol flare analysed in the previous subsection. Besides the absolute values of the count rate which is by a factor of 500 higher for Algol (note, that the observations were performed by different instruments and, therefore, the differences in count rate are no direct measure for the differences in flux), the shape of the SR 13 flare is very similar to that of the flare on Algol.

The rotational period of the CTTS SR 13 is unknown to the present. We determined the quiescent emission of SR 13 from the pre-flare data of the first satellite orbit. Our attempt to find the rotational period from the modeling of the flare according to Eq. (3) with $P_{\rm rot}$ a free parameter failed, since the uncertainties in the data do not allow to distinguish between different fit solutions. In Fig. 5a we overlay the data points by two solutions of the 'rotating-flare model', one was found assuming a period of 3 d, the other one corresponds to twice that period.

A detailed spectral analysis of this specific flare event similar to the one carried out for the Algol flare (see Stern et al. 1992 and Sect. 4.1) is not practicable due to the low number of counts. To underline the difficulty in evaluating the spectral information for the flare on SR 13, we briefly discuss the results from our attempts to fit a Raymond-Smith model (Raymond & Smith 1977) to the spectra during four stages of the flare that were defined in the following way: phase 1 is given by the quiescent stage, phase 2 is the observed, *apparent* flare rise, and phases 3 and 4 correspond to the observed decay. The three flare time intervals are marked in Fig. 5a. The quiescent spectrum was computed from an earlier observation obtained in 1991 March 05–10 by the *ROSAT* PSPC due to the scarcity of non-flare data in the September observation.

A two-temperature Raymond-Smith model was needed to obtain acceptable fits with $\chi^2_{\rm red} < 1.4$ for each of the four phases, where we held the temperature of the softer component fixed at $kT = 0.25\,{\rm keV}$. The graphs in Fig. 5c and d display the best fit values for the temperature and emission measure of the hotter component. The large uncertainties of the best fit values shown in Table 2 prohibit a spectral study with better time resolution, but having only four time bins to define the spectral evolution, the decay of the emission measure after the flaring volume became visible could not be pinned down, and thus a check of the 'rotating flare model' by modeling of the time development of the emission measure is not possible for this flare on SR 13. A slight indication for cooling is present in the evolution of kT during the flare suggesting that the actual outburst might in fact have occurred as early as during the second phase.

In cases of insufficient data quality hardness ratios may be used to give a clue to spectral properties. Neuhäuser et al. (1995) showed that the *ROSAT* hardness ratio *HR2* (see Neuhäuser et al. 1995 for a definition) is related to the temperature of the plasma (see their Fig. 4). We computed *HR2* for the four different time intervals defined above. The time evolution of the hardness ratio *HR2* is displayed in Fig. 5b. The decreasing *HR2* during the last three intervals supports the decline in temperature measured in the spectra and presents further evidence for cooling.

To conclude, the results on the SR 13 lightcurve, while having an admittedly reduced statistical significance, are fully consistent with an interpretation in terms of flare cooling combined with rotational modulation.

4.3. P1724

The *ROSAT* HRI observation of P1724 comprises 13 satellite orbits (see Fig. 6). Similar to the flare on SR 13, constant count rate is observed only during the very first orbit. We, therefore, base our value for the quiescent emission, $0.04\,{\rm cps}$, on this time interval and find that it is consistent with most of the observations of P1724 presented by Neuhäuser et al. (1998). However, in March 1991 the count rate was higher by a factor 4, possibly indicating long-term variations in the quiescent emission.

The lightcurve during the second orbit resembles a small flare event and is omitted from our analysis. The maximum of the large flare that dominates this observation extends over

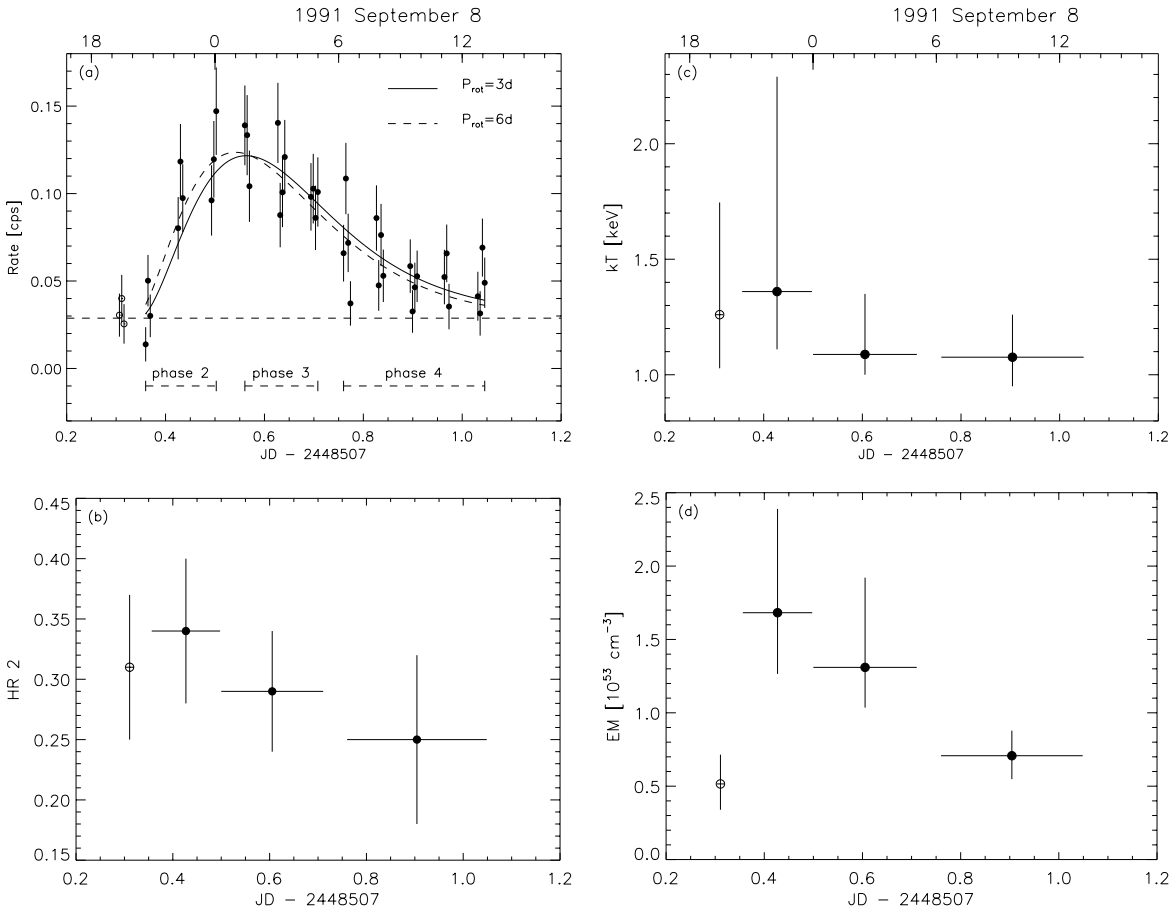

Fig. 5a–d. *ROSAT* PSPC observation of a flare on SR 13: **a** X-ray lightcurve (400 s bins, 1 σ uncertainties) and best fit model. Data used in the fitting process are represented by filled circles. Open circles are pre-flare data. **b** Time evolution of the hardness ratio *HR2* during the flare on SR 13. Note, that the first value (open circle) was determined from the data of a 1991 March observation and is plotted here at an arbitrary time prior to the flare. Time dependency of the temperature **c** and emission measure **d** of a Raymond-Smith model spectrum display large uncertainties (shown are 90 % confidence levels).

almost 4 hours. During the decline of the count rate irregular variations are observed that might be due to short timescale activity superposed on the large flare event. We ignore these fluctuations and model the lightcurve beginning after the second data gap by Eq. (3).

The total number of source counts measured in this observation is smaller than 1000, and thus far too low for a timesliced hardness ratio analysis. Having in view the similarity between the X-ray lightcurve of this flare and the previously discussed flares, and the good description of the data by our best fit, we trust that the 'rotating flare model' applies also to this observation.

4.4. V773 Tau

An intense X-ray flare on V773 Tau has been reported by Skinner et al. (1997) and interpreted as a sinusoidal variation whose period is approximately equal to the known optical period of V773 Tau, i.e. 71.2 h.

The *ASCA* lightcurve of this event (see Fig. 7) is characterized by constant count rate at maximum emission which lasts

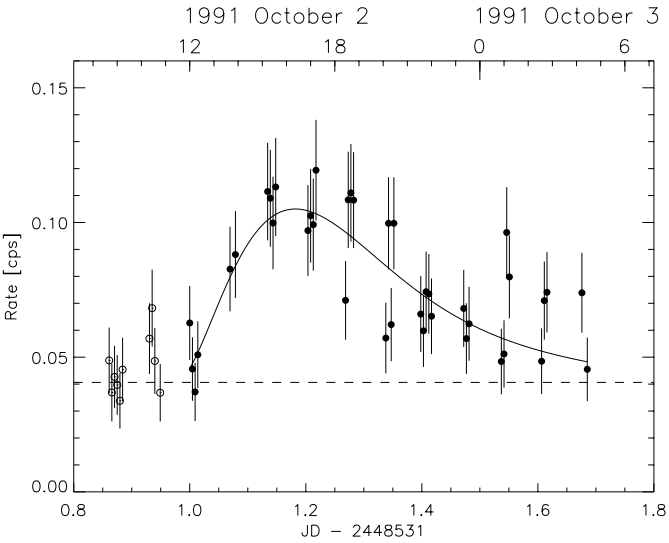

Fig. 6. *ROSAT* HRI lightcurve of the flare on P1724 (400 s bins, 1 σ uncertainties) and best fit model. The meaning of the plotting symbols is the same as in Fig. 5

over more than 2 h making the event a candidate for a rotationally modulated flare. No data is available prior to the peak emission, but observations resumed about 10 h after the maximum and display a steady decrease in count rate. Since the pre-flare stage and the rise of the flare are completely missing in the data, the flare volume must have emerged from the backside of the star well before the start of the observation, and an additional time offset parameter δt has to be included in the fit (analogous to the modeling of the flare on Algol), to determine the time that elapsed between phase $\pi - \phi_{\rm crit}$ (= emergence of the flare volume) and the first measurement.

Since the flare covers the complete observation a value for the quiescent count rate, $I_{\rm q} = 0.10 \pm 0.02$ cps, was adopted from a later ASCA SIS0 observation in February 1996, also presented by Skinner et al. (1997). Despite the fact that the broad maximum of the September 1995 lightcurve can be explained by the loop rotating into the line of sight, no satisfying fit could be obtained for the flare on V773 Tau by the model of Eq. (3) even after a time offset δt was added ($\chi^2_{\rm red} = 2.51$ for 149 degrees of freedom): The decay of the observed lightcurve seems to be faster than our model predictions (see Fig. 7 dotted curve). We note that the data is slightly bended towards the time axis around the 6th data interval after the start of the observation. This behavior, producing an overall 'convex' shape of the X-ray lightcurve, could be due to an additional feature on the surface of the star. We suggest that a localized region with enhanced X-ray emission can be responsible for this break if this region disappears due to the star's rotation at $\sim$ JD 2449977.85. For comparison we show a fit of our 'rotating flare model' where such a feature has been included (solid line in Fig. 7, $\chi^2_{\rm red} = 1.47$ for 149 degrees of freedom). Since we are interested in a qualitative description of the shape of the lightcurve only we assumed that this region makes up for 0.2 cps during its visibility and begins to disappear gradually at JD 2449977.85. Representing this X-ray emitter by another set of *free* parameters would certainly further improve the already good agreement between data and model.

Skinner et al. (1997) also present the time behavior of the emission measure derived from a two-temperature fit to the *ASCA* spectrum. If our interpretation of adding a soft X-ray spot, which gradually rotates away, is correct, then the emission measure of the soft component should stay constant for most of the time, but decrease towards the end of the observation. However, the S/N of the time-sliced spectral fits (Skinner et al. 1997, his Fig. 10, middle panel) is not sufficient to judge whether this is indeed the case.

To conclude, other interpretations such as a different kind of anomalous flaring cannot be excluded from the data of this observation. Tsuboi et al. (1998) have presented another *ASCA* flare observation of V773 Tau. In that observation V773 Tau shows the typical flare behavior in the sense of a sharp rise and a subsequent longer decay of count rate, temperature, and emission measure. However, their attempt to fit an e-folding decay to the lightcurve of the hard X-ray count rate was not successful the count rate remaining too high towards the end of the observation. Hence, unusually long decays seem to be characteristic for V773 Tau.

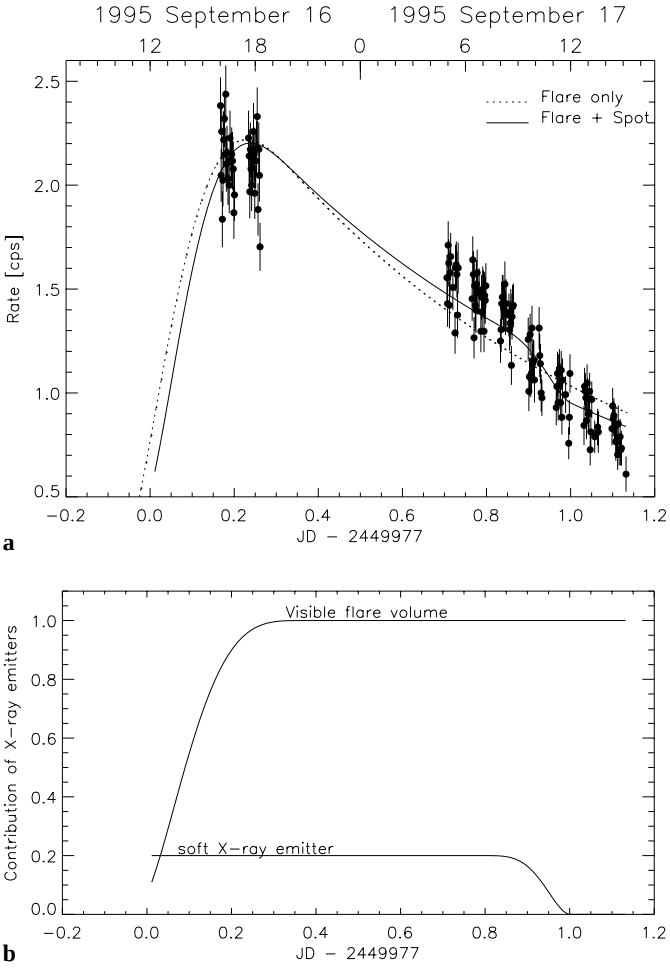

Fig. 7. a *ASCA* lightcurve of the observation of V773 Tau (128 s bins, $1\,\sigma$ uncertainties) and best fit. Modeling of a rotating flare alone (dotted line) does not lead to an acceptable fit, while adding an additional feature producing enhanced X-rays until JD 2449977.85 and then gradually disappearing describes the bending of the lightcurve and improves the fit perceptibly (solid line). **b** Time evolution of the visible flare volume and the secondary X-ray emitter during the flare on V773 Tau as found from the best fit of the 'rotating-flare model' to the lightcurve.

5. Summary and conclusions

We have presented a sample of four untypical flare events and provided a common explanation: Parameters that depend on the size of the emitting plasma volume (e.g. count rate, EM) deviate from the standard exponential decay behavior due to temporary occultation of the flaring volume by the rotating star. This is most evident from the large flare on Algol, for which the data are most abundant and our modeling is therefore most reliable.

The comparatively slow rise of the count rate in the X-ray lightcurve, broad maxima and following exponential decay are well represented by a model that describes emission from a spherical plasma loop that emerges from the back of the star

and gradually rotates into the line of sight of the observer. The increasing visible fraction of the loop produces the flat maximum and apparent slow-down of the rise stage.

In our data there is no indication for sine-like modulation of the X-ray lightcurve, since all but one of the lightcurves are clearly asymmetric, and the duration of all events is well below the rotational period of the host star. The only exception is the flare on V773 Tau where Skinner et al. (1997) proposed sinusoidal modulation to reproduce the shape of the *ASCA* lightcurve. We suggest a different explanation involving a second X-ray emitting region on the star additionally to a rotationally modulated flare to come up for the 'convex' shape of the lightcurve. However, due to the lack of pre-flare data, no conclusive evidence is present for either of the interpretations. Evidence for reheating of the plasma at $\sim \mathrm{JD}2449978.05$ inferred from the increase of the hardness ratio (see Skinner et al. 1997) does not contradict our model, but could be related to the disappearing of a region emitting soft X-rays similar to the one we introduce. No significant change in temperature nor emission measure of the soft component was observed in Skinner's spectral analysis, but we note that the results of spectral fitting depend on the assumption for the abundances and column density.

The decay timescales τ found from our best fit to the respective flare event are all in the typical range for TTS flares (of a few hours) except for V773 Tau, where the flare lasted extraordinary long ($> 20\,\mathrm{h}$). Comparatively large loop sizes of a considerable fraction of the radius of the star are obtained for all observations analysed here, r spanning between 10 to 65 % of the star radius. These values are in agreement with typical loop sizes for TTS flares inferred from quasi-static loop modeling (see Montmerle et al. 1983, Preibisch et al. 1993).

In view of the large relative size of the ratio between loop and star radius the assumptions we explain in Sect. 3 concerning our model for a rotating flare might seem somewhat oversimplifying. We also note that different solutions of the model seem to describe the data equally well even in the case of the well restrained Algol observation. Therefore, uncertainties in the fit parameters are to be regarded carefully. However, the qualitative description of the scenario is very good and the data are well represented by the model. Other interpretations of the 'anomalous' flare events we presented in this paper may not be excluded but are still to be traced.

Clearly, continuous observations of whole flares are needed to verify whether an event could be subject to rotational modulation of the kind we discussed in this paper. Up to date most of the flares observed lack completeness in that either the rise or part of the decay were missed by the observation. In the near future *XMM* will provide the possibility of long, uninterrupted observations (up to $\sim 25\,\mathrm{h}$) that will enable to pursue the development of flares in whole. Better statistics are needed to be able to study the time development of spectral parameters for TTS flares, and try to confirm the 'rotating flare model' by use of the spectral information similar to our analysis of the Algol observation.

Acknowledgements. We would like to thank R. Stern and S. Skinner who provided us the *Ginga* and *ASCA* data. The *ROSAT* project is supported by the Max-Planck-Gesellschaft and Germany's federal government (BMBF/DLR). RN acknowledges grants from the Deutsche Forschungsgemeinschaft (Schwerpunktprogramm 'Physics of star formation').

References

Casanova S., 1994, Ph.D. Thesis, University Paris 7
Cutispoto G., Tagliaferri G., Pallavicini R., et al., 1996, A&AS 115, 41
Damiani F., Micela G., Sciortino S., 1994, In: Zimmermann H.U., Trümper J. E., Yorke H. (eds.) X-rays from the universe. MPE report 263, Max-Planck-Institut für Extraterrestrische Physik, Garching, p. 28
Ghez A.M., Neugebauer G., Matthews K., 1993, AJ 106, 2005
Grosso N., Montmerle T., Feigelson E.D., et al., 1997, Nat 387, 56
Haisch B., Strong K.T., Rodono M., 1991, ARA&A 29, 275
Heise J., Brinkman A.C., Schrijver J., et al., 1975, ApJ 202, L73
Hill G., Barnes J.V., Hutchings J.B., et al., 1971, ApJ 168, 443
Lampton M., Margon B., Bowyer S., 1976, ApJ 208, 177
Montmerle T., 1997, In: Micela G., Pallavicini R., Sciortino S. (eds.) Mem. Soc. Astron. Ital. Vol. 68, No.4, Soc. astron. Ital., Firenze, p. 1017
Montmerle T., Koch-Miramond L., Falgarone E., et al., 1983, ApJ 269, 182
Neuhäuser R., Sterzik M.F., Schmitt J.H.M.M., et al., 1995, A&A 297, 391
Neuhäuser R., Wolk S.J., Torres G., et al., 1998, A&A 334, 873
Ottmann R., Schmitt J.H.M.M., 1996, A&A 307, 813
Pettersen B.R., 1989, Solar Physics 121, 299
Preibisch T., Zinnecker H., Schmitt J.H.M.M., 1993, A&A 279, L33
Preibisch T., Neuhäuser R., Alcala J.M., 1995, A&A 304, L13
Raymond J.C., Smith B.W., 1977, ApJS 35, 419
Rydgren A.E., Vrba F.J., 1983, ApJ 267, 191
Skinner S.L., Güdel M., Koyama K., et al., 1997, ApJ 486, 886
Stern R.A., Haisch B.M., Nagase F., et al., 1990, In: Wallerstein G. (ed.) Cool stars, stellar systems, and the sun. Proc. of the 6th Cambridge Workshop, Astron. Soc. Pacific, San Francisco, p. 224
Stern R.A., Uchida Y., Tsuneta S., et al., 1992, ApJ 400, 321
Tanaka Y., Inoue H., Holt S.S., 1994, PASJ 46, L37
Trümper J., 1982, Adv. Space Res. 2 (no.4), 241
Tsuboi Y., Koyama K., Murakami H., et al., 1998, ApJ 503, 894
Turner M.J.L., Thomas H.D., Patchett B.E., et al., 1989, PASJ 41, 345
van den Oord G.H.J., Mewe R., 1989, A&A 213, 245
Welty A.D., 1995, AJ 110, 776
Zimmermann H.U., Becker W., Izzo C., et al., 1995, EXSAS Handbook, Garching